Blue TADF Emitters Based on Indenocarbazole Derivatives with High Photoluminescence and Electroluminescence Efficiencies

Xialei Lv,† Rongjuan Huang,‡ Shuaiqiang Sun,† Qing Zhang,† Songpo Xiang,† Shaofeng Ye,† Panpan Leng,† Fernando B. Dias,*,‡ and Lei Wang*,†

† Wuhan National Laboratory for Optoelectronics, Huazhong University of Science and Technology, Wuhan, 430074, P. R. China
‡ Physics Department, Durham University, South Road, Durham DH1 3LE, UK

Abstract:

A series of blue thermally activated delayed fluorescence (TADF) emitters were designed and synthesized, using 2,4,6-triphenyl-1,3,5-triazine as the acceptor unit, and indenocarbazole derivatives as the electron-donating moiety. In contrast with other six-membered heterocycles, like phenothiazine, phenoxazine and dihydroacridine, where the TADF efficiency is affected by the presence of different conformers, indenocarbazole derivatives do not show this effect. Therefore, **InCz23FlTz, InCz23DPhTz, InCz23DMeTz** and **InCz34DPhTz** allow to investigate the influence of different substituents and substitution positions on TADF properties, without the difficulty of having to deal with changes on conformation. We demonstrate that the substituted position on the carbazole and different substituents in the same position have clear influence on the donor character of indenocarbazole derivatives. Also, the color purity of blue emission and excited states could be adjusted by substituents and substituted position, thus excellent blue emitters can be obtained. Besides, the four compounds show relatively small TADF contribution under optical excitation, however excellent performances are obtained in the electroluminescent devices, especially with **InCz34DPhTz**, which shows a maximum external quantum efficiency (EQE) around 26%. In the end, we find an effective way to design high efficiency blue TADF materials and deeply study the relation between structure and property in indenocarbazole derivatives.

Keywords: *thermally activated delayed fluorescence (TADF), indenocarbazole derivatives, substituted position, substituents, photophysical properties.*

Introduction:

Organic light-emitting diodes (OLEDs) are electroluminescent devices, which can be used to fabricate lighter, thinner and flexible displays, with faster time response, higher contrast, lower power consumption and no need for backlight, with bring significant cost savings over liquid crystal display (LCD). Therefore, OLEDs represent the future trend on displays and lighting technologies and attracts more and more attention from industry and scientific research circles. [1-2] Nevertheless, the design of highly efficient blue emitters is still challenging as these compounds often suffer from pronounced degradation upon excitation on account of its intrinsically high energy levels.[3] Moreover, as the excitons are made of singlet and triplet character, formed in a ratio of 1:3 under electric injection, according to the spin-statistic model, and triplets are often not emissive, OLEDs containing pure fluorescent materials can only use singlet excitons. The internal quantum efficiency of traditional fluorescent OLEDs (IQE) is thus limited to 25%. OLEDs using phosphorescent materials, containing heavy metals, and thermally activated delayed fluorescence (TADF) molecules can reach 100% IQE in theory, due to the possibility of using both singlet and triplet excitons in the radiative process. However, the operational lifetime of most blue phosphorescent OLEDs is particularly short, often less than one tenth of the lifetime of conventional blue fluorescent OLEDs, mainly due to the degradation of the blue emitter.[4] Recently, the development of high efficiency blue TADF materials appeared as a promising alternative to blue phosphorescent emitters and a viable alternative to pure fluorescent emitters, however the design of stable and highly efficient blue TADF emitters is still challenging.[5-8]

Efficient thermal activated conversion of triplet to singlet excitons in TADF materials is usually realized in molecules showing charge-transfer (CT) states, featuring well separated highest occupied molecular orbital (HOMO) and lowest unoccupied molecular orbital (LUMO) that result in very small singlet-triplet energy gap.[9] On base of Fermi's golden rule, a large rate of reverse intersystem crossing (RISC) not only needs a small ΔE_{ST} (the energy gap between the lowest singlet excited state (S_1)

and the lowest triplet excited state (T_1), but also an enhanced spin-orbital coupling (SOC) between the S_1 and T_1 (or upper T_n, $n \geq 2$).[10] Whereas, a small ΔE_{ST} is often presented in molecules with charge transfer states and twisted structure, a fast non-radiative internal conversion rate can be a strong competitor with the RISC rate and the radiative rate from S_1, which end-up diminishing the efficiencies of delayed luminescence. Therefore, it is of great importance to achieve a high photoluminescence quantum yield (PLQY) and a small ΔE_{ST} simultaneously, when designing TADF materials.[11]

Many excellent TADF materials have emerged in the last five years, with satisfying performances in the green region mainly, yet stable and high efficiency blue TADF emitters still face many problems.[12-13] Carbazole is a low-cost material, with a high triplet energy (T_1 = 3.0 eV) and efficient hole-transporting ability, and its derivatives are popularly applied in blue OLED materials.[14-15] For example, Guo and co-workers designed an indenocarbazole derivative (DPDDC) with a small ΔE_{ST} but low PLQY, which was used as host in phosphorescent OLEDs, and achieved a high external quantum efficiency (EQE) of 23.6%, with low current efficiency roll-off and a twentyfold device lifetime improvement over the reference electrophosphorescent device.[16] Chi and co-workers performed a systematic investigation of structure-property correlation in a series of indolo[3,2-b]indole (IDID) derivatives, substituted with various acceptor (A) moieties.[17] They clearly indicated that indenocarbazole can feature high hole mobility and a low-lying local excited (LE) triplet state owing to its planar rigid backbone. However, to the best of our knowledge, rare studies were carried out regarding the effect on the TADF properties of indenocarbazole with different substituents.[18-21] Here, we conduct an investigation on the TADF properties of a series of indenocarbazole derivatives substituted at the 2,3 positions on carbazole with different substituents, fluorene (Fl), diphenyl (DPh) and dimethyl (DMe), identified as **InCz23FlTz**, **InCz23DPhTz**, and **InCz23DMeTz**, respectively, and using the same substituent DPh but substituted at the 3,4 positions, also on carbazole, named **InCz34DPhTz**. Among which, **InCz23FlTz** was studied

before named **SFI23pTz**.[22] The modified indenocarbazoles were chosen as donor groups due to their rigid structure, promising to show larger conformation stability when compared with other six-membered heterocycles, like phenothiazine, phenoxazine and dihydroacridine.[23-25] 2,4,6-Triphenyl-1,3,5-triazine is used as the acceptor unit and is unaltered, since it is chemically stable.[26]

The position of substitution on carbazole and substituted groups of the indenocarbazole derivatives all have influence on the TADF properties studied here. The four compounds show obvious TADF phenomena, evaluated from optical measurements such as comparing degassed *vs* aerated steady state luminescence spectra, time resolved fluorescence decays collected at different temperatures, and the power dependence of the delay emission intensity. However, the contribution of TADF to the overall emission is relatively small under optical excitation, and strong PLQY is observed in these compounds. This is consistent with the relatively large singlet and triplet gap (~0.2 eV) and slow reverse intersystem crossing rate (~10^4 s^{-1}). Surprisingly, when compared with the TADF contribution obtained in photoluminescence, the electroluminescence devices performed excellently for all compounds due to their large PLQY, which balances the less efficient triplet harvesting. Therefore, this paper offers a new strategy to design high effective blue TADF materials.

■ Experimental section

General Method

The raw materials and related solvents used in the synthesis process were used as supplied without further purification unless other is stated. Since the solubility of the four materials are not good, the crude product of the target compounds were purified by column chromatography on silica gel firstly, then recrystallization treatment, finally sublimation by programmed gradient heating. The structure of the immediate compounds was confirmed by ^{1}H NMR and mass spectra, and ^{13}C NMR spectra and elemental analyses were also measured for final products. The thermal decomposition temperatures (T_d) and glass transition temperature (T_g) were measured to evaluate the

thermal properties. The UV-vis absorption spectra, PL spectra, absolute PLQYs (excited at 360 nm) and electrochemical properties studied by cyclic voltammetry (CV), were investigated as described in previous publication.[22] The lifetimes of delayed fluorescence were obtained by collecting the time-resolved spectra, using a Nd: yittrium aluminium garnet (YAG) laser (EKSPLA), 10 Hz, 355 nm as the excitation source. The luminescence was collected through a spectrograph and a gated intensified charged couple device (iCCD) camera (Stanford Computer Optics). The power dependence measurements were done using a nitrogen laser, 10 Hz, 337 nm as the excitation source.[25]

Calculation details

The geometrical and electronic properties of the ground-state and the excited states (S_1 and T_1) were all optimized as described in the previous reported publication.[22]

Device fabrication and measurement

The preparation of indium tin oxide, the device fabrication process and the determination of the EQE values were also done as described previosuly.[27]

Synthesis

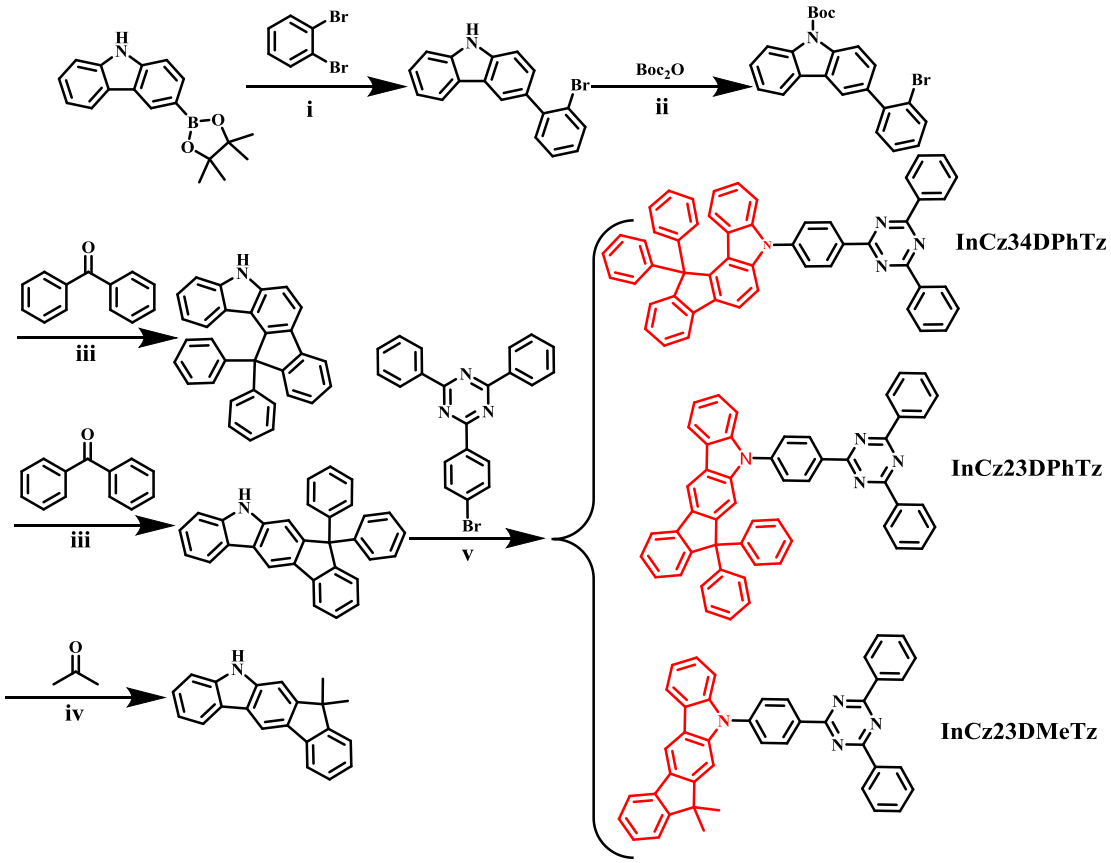

Scheme 1. Synthetic routes: (**i**) K_2CO_3, $Pd(PPh_3)_4$, toluene, ethanol, 100 ˚C, 12h, N_2; (**ii**) $B_{OC2}O$, 4-dimethylaminopyridine, THF, room temperature, 4h, air; (**iii**)/(**iv**) *n*-BuLi, THF, -78 ˚C, 12h, N_2; HOAc, HCl, 120 ˚C, 4 h, air; (**v**) $Pd(OAc)_2$, P(*t*-Bu)$_3$.HBF_4, NaO*t*Bu, toluene, 110 ˚C, 4h, N_2.

The detailed synthesis process

***Synthesis of compound* 3-(2-bromophenyl)-9*H*-carbazole:** The synthesis was referred to the reported paper.[22]

Synthesis of compound tert*-butyl 3-(2-bromophenyl)-9*H*-carbazole-9-carboxylate*: The di-*tert*-butyl dicarbonate (26.56 g, 121.72 mmol) and 4-dimethylaminopyridine (1.06 g, 8.694 mmol) were added into to a three-neck round bottom flask, and stirred with tetrahydrofuran (THF, 100 mL). Then, 3-(2-bromophenyl)-9*H*-carbazole (28 g, 86.94 mmol) was added into the stirred solution at room temperature and stirred for 4 hours. Firstly, the THF was removed under vacuum. Then, the intermediate product was obtained as a white powder by column chromatography on

silica gel (yield: 98%). ^{1}H NMR (400 MHz, $CDCl_3$) δ [ppm]:8.36-8.32 (t, *J* = 8.0 Hz, 2H), 8.27-7.93 (m, 2H), 7.72-7.70 (d, *J* = 8.0 Hz, 1H), 7.56-7.24 (m, 5H), 7.22-7.18 (m, 1H), 1.78-1.74 (d, *J* = 16.0 Hz, 9H). MS (mass spectrum) (ESI): calcd for $C_{23}H_{20}BrNO_2$: 421.0677; found: 444.0571 $[M+Na]^+$.

***Synthesis of compound* 12,12-diphenyl-5,12-dihydroindeno[1,2-*c*]carbazole *and* 7,7-diphenyl-5,7-dihydroindeno[2,1-*b*]carbazole:** The reaction process was referred to the previous paper.[22] The product was further purified by silica gel column chromatography and two isomers were obtained.

12,12-diphenyl-5,12-dihydroindeno[1,2-*c*]carbazole (yield: 40%): ^{1}H NMR (400 MHz, $CDCl_3$) δ [ppm]: 8.21 (s, 1H), 7.93-7.91 (d, *J* = 8.0 Hz, 1H), 7.75-7.73 (d, *J* = 7.2 Hz, 1H), 7.60-7.40 (m, 7H), 7.34-7.30 (t, *J* = 7.4 Hz, 2H), 7.17-7.15 (m, 8H), 6.85-6.84 (t, *J* = 3.4 Hz, 1H). MS (APCI): calcd for $C_{31}H_{21}N$: 407.1674; found: 408.1748 $[M+H]^+$.

7,7-diphenyl-5,7-dihydroindeno[2,1-*b*]carbazole (yield: 35 %): ^{1}H NMR (400 MHz, $CDCl_3$) δ [ppm]: 8.42 (s, 1H), 8.14-8.12 (d, *J* = 7.6 Hz, 1H), 7.94 (s, 1H), 7.88-7.86 (d, *J* = 7.6 Hz, 1H), 7.41-7.36 (m, 5H), 7.26-7.21 (m, 12H). MS (APCI): calcd for $C_{31}H_{21}N$: 407.1674; found: 408.1746 $[M+H]^+$.

***Synthesis of compound* 5-(4-(4,6-diphenyl-1,3,5-triazin-2-yl)phenyl) -12,12-diphenyl-5,12-dihydroindeno[1,2-*c*]carbazole (InCz34DPhTz):** The synthesis process was referred to reported paper (yield: 80%).[22] ^{1}H NMR (400 MHz, $CDCl_3$) δ [ppm]: 9.07-9.05 (d, *J* = 8.4 Hz, 2H), 8.89-8.87 (m, 4H), 7.96-7.94 (d, *J* = 8.4 Hz, 1H), 7.85-7.80 (t, *J* = 9.8 Hz, 3H), 7.69-7.60 (m, 11H), 7.51-7.24 (m, 12H), 7.00-6.98 (m, 1H). ^{13}C NMR (100 MHz, $CDCl_3$) δ [ppm]: 171.86, 170.94, 153.84, 147.00, 141.56, 141.41, 141.23, 141.15, 140.41, 136.14, 135.39, 134.03,

132.73, 130.68, 129.08, 128.75, 128.21, 127.55, 127.39, 126.78, 126.50, 125.85, 125.60, 125.51, 122.44, 121.27, 119.75, 119.02, 118.41, 109.95, 109.41, 66.09. MS (APCI): calcd for $C_{52}H_{34}N_4$: 714.2783; found: 715.2852 $[M+H]^+$.

***Synthesis of compound* 5-(4-(4,6-diphenyl-1,3,5-triazin-2-yl)phenyl) -7,7-diphenyl-5,7-dihydroindeno[2,1-*b*]carbazole (InCz23DPhTz):** The synthesis of **InCz23DPhTz** was referred to that of **InCz34DPhTz**. ^{1}H NMR (400 MHz, $CDCl_3$) δ [ppm]: 8.96-8.94 (d, *J* = 8.4 Hz, 2H), 8.81-8.80 (d, *J* = 6.8 Hz, 4H), 8.50 (s, 1H), 8.23-8.21 (d, *J* = 8.0Hz, 1H), 7.92-7.90 (d, *J* = 7.6 Hz, 1H), 7.72-7.70 (d, *J* = 8.4 Hz, 2H), 7.63-7.33 (m, 12H), 7.25-7.28 (m, 11H). ^{13}C NMR (100 MHz, $CDCl_3$) δ [ppm]: 171.81, 170.91, 151.03, 150.72, 146.55, 141.47, 141.07, 140.74, 140.52, 136.13, 134.85, 133.70, 132.67, 130.62, 129.03, 128.72, 128.27, 128.22, 127.59, 126.90, 126.59, 126.55, 126.23, 126.16, 123.82, 123.76, 120.61, 120.39, 119.59, 111.54, 110.01, 107.81, 65.51. MS (APCI): calcd for $C_{52}H_{34}N_4$: 714.2783; found: 715.2850 $[M+H]^+$.

***Synthesis of compound* 7,7-dimethyl-5,7-dihydroindeno[2,1-*b*]carbazole:** The synthesis was referred to the preparation of the compound 12,12-diphenyl-5,12-dihydroindeno[1,2-c]carbazole and 7,7-diphenyl-5,7-Dihydro-indeno[2,1-b]carbazole. One of the raw materials benzophenone was replaced by anhydrous acetone (yield: 39%). ^{1}H NMR (400 MHz, $CDCl_3$) δ [ppm]: 8.38 (s, 1H), 8.14-8.12 (d, *J* = 7.6 Hz, 1H), 8.06 (s, 1H), 7.84-7.82 (d, *J* = 7.2 Hz, 1H), 7.44-7.35 (m, 6H), 7.30-7.23 (m, 1H), 1.71-1.56 (m, 6H). MS (APCI): calcd for $C_{21}H_{17}N$: 283.1361; found: 284.1434 $[M+H]^+$.

***Synthesis of compound* 5-(4-(4,6-diphenyl-1,3,5-triazin-2-yl)phenyl) -7,7-dimethyl-5,7-dihydroindeno[2,1-*b*]carbazole (InCz23DMeTz):** The synthesis method is the same as **InCz23DPhTz**. ^{1}H NMR (400 MHz, $CDCl_3$) δ [ppm]: 9.08-9.06 (d, *J* = 8.4 Hz, 2H), 8.85-8.83, 8.77-8.76 (dd, *J* = 6.8 Hz, *J* = 4.0 Hz, 4H), 8.46 (s, 1H), 8.23-8.21 (d, *J* = 7.6 Hz, 1H), 7.88-7.86 (d, *J* = 8.0 Hz, 3H), 7.74-7.55 (m, 8H), 7.45-7.28 (m, 5H), 1.56-1.54 (m, 6H). ^{13}C NMR (100 MHz, $CDCl_3$) δ [ppm]: 171.86, 140.90, 139.58, 136.13, 132.71, 130.74, 129.03, 128.74, 127.08, 126.90, 126.42, 125.84, 122.58, 120.44, 119.42, 111.42, 109.94, 104.10, 46.84, 27.94. MS (APCI): calcd for $C_{42}H_{30}N_4$: 590.2470; found: 591.2600 $[M+H]^+$.

■ Results and discussion

Synthesis and thermal stability

A series of indenocarbazole derivatives with rigid and twisted structure were designed and synthesized to promote simultaneously triplet harvesting trough thermally activated RISC and maintaining strong PLQY. Different substituted groups and substitution positions on carbazole merely alter the degree of electronic delocalization, and appear not influencing the triplet energy due to the similar conjugation degree. However, these substitutions affect the singlet energy levels. The triphenyltriazine (Tz) is chosen as the acceptor in the four TADF molecules studied here. Inserting a phenyl group between the donor and acceptor aimed to increase slightly the overlap between HOMO and LUMO in order to achieve high PLQY, while keeping blue emission.[28-30] In short, it will be of significance for the future molecular design to study the relationship among the molecular structure and the photophysical and electroluminescence properties. Additionally, the synthesis of all the target compounds included Suzuki Coupling reaction, lithium-bromine exchange reaction, Buchwald-Hartwig coupling reaction and so on as shown in **Scheme 1**. Details of the preparation and structural characterizations are provided in the experimental section. From the thermal stability measurement as shown in **Figure S1**, it was found that all four compounds show excellent thermal stability with temperatures of decomposition (T_d) beyond 436 ^{o}C except **InCz23DMeTz** (374 ^{o}C). **InCz23DPhTz** shows no obvious T_g between 50-250 ^{o}C (as seen in **Figure S1**), and the other three compounds exhibit glass transition temperatures (T_g) between 170-181 ^{o}C, which make them more likely to form high-stable films through vacuum evaporation.

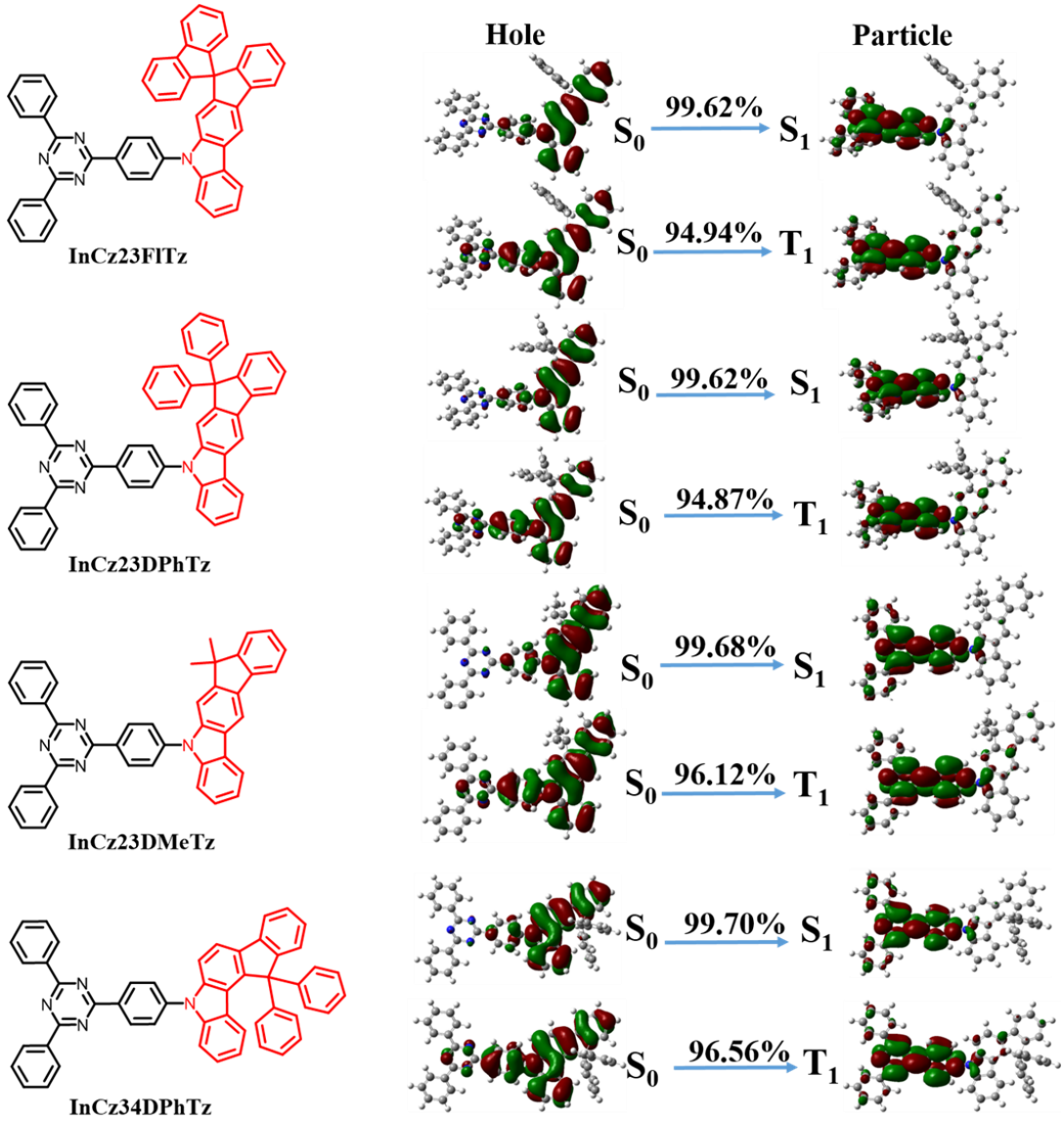

Figure 1. Molecular configurations, and the NTO calculation for **InCz23FlTz**, **InCz23DPhTz**, **InCz23DMeTz** and **InCz34DPhTz.**

Theory Calculations.

The electron density distributions of the ground state were investigated using density functional theory (DFT) calculations at the B3LYP/6-31G level. As shown in **Figure S2**, the HOMO is mainly located on the carbazole group, extending to the adjacent indole and partly to the central phenyl, yet there was no contribution from the substituted groups on indole. Whereas, the LUMO distributions were almost the same for all the four compounds, localized on the Tz acceptor and partly extended to the

phenyl spacer. The HOMO/LUMO energy levels of the donors were calculated as displayed in **Table 1**. As seen in **Table S1**, although there was almost no electron distribution on the side units, the HOMO and LUMO electron distribution and energy levels were affected subtly by the substituent and substituted position**.** As the substituent on indole changes from fluorene (Fl), to diphenyl (DPh), and to dimethyl (DMe) in the same substituted position, the HOMO gets increasingly shallower due to the electron-donating ability in the order of fluorene < diphenyl < dimethyl. For the same substituent DPh, 3, 4 substituted on carbazole has stronger electron-donating capacity than that of 2, 3 position since the HOMO is shallower than that of 2, 3 position, which coincides with the consequence that we have studied 3,4 position of carbazole substituted with spirobifluorene has stronger electron-donating ability than 2,3 position.[22] The different substituent groups and positions on carbazole appear to change the strength of the intramolecular charge transfer (ICT) states, yet holding similar high triplet energy levels, probably because of the similar overlap of the FMOs. The similarly separated HOMO and LUMO orbitals, and the distorted structures ensure a small energy gap between the S_1 and T_1 states. The natural transition orbital (NTO) method was used to explore the transition characteristics (as seen in **Figure 1**), and revealed typical CT singlet (S_1) excited states with "hole" and "particle" localized on the indenocarbazole and Tz, respectively. As for the nature of triplet (T_1), they are mainly CT character with small contributions of locally excited (LE) states. Based on recent studies, a vibronic coupling process occurring between ^{3}CT and ^{3}LE states assists the RISC mechanism and promotes the spin-flip back to the ^{1}CT state, which favors the SOC process between the ^{1}CT and ^{3}LE states.[9, 31-34] The calculated energy gaps were in the range of 0.21-0.25 eV, which was larger than in most reported blue materials.[35] The experimental values of HOMO/LUMO of the four compounds were investigated by cyclic voltammetry (CV) with the traditional three-electrode system. As seen in **Figure S3**, all the compounds showed similar reduction potentials with a very small fluctuation. However, with the substituent changing from fluorene, to diphenyl, to dimethyl, the oxidation potential is clearly

reduced.[36] The detailed energy levels are shown in the device structures in the electroluminescence part.

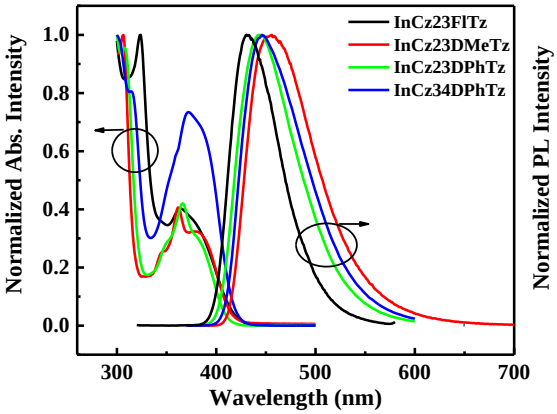

Figure 2. The UV-vis absorption and PL emission spectra of the compounds in toluene solution.

Photophysics. Figure 2, shows the absorption and photoluminescence (PL) spectra of the four compounds in dilute toluene solutions, measured at 298 K. The absorption peaks in the short-wavelength region, around 309-324 nm, are the signature of the π-π* transition in the indenocarbazole moieties. The absorption bands in the 362-372 nm interval can be ascribed to the entire conjugated backbone. The emission of all four compounds in toluene show Gaussian-type band shape, consistent with the CT character of the excited state.[36] Fluorene imposes more restriction to rotation possibility than diphenyl, and dimethyl has the maximum freedom to rotate. For the same substituent, the 2, 3 positions have stronger steric effect than 3, 4 substituted on carbazole. The FWHM is related to the strength of ICT state, and increases from 57nm (**InCz23FlTz**), 69 nm (**InCz23DPhTz**), 73 nm (**InCz34DPhTz**), and 79 nm (**InCz23DMeTz**). The substituents and substituted positions also influence the color purity. Moreover, the emission properties are strongly affected by the polarity of the local environment, as seen from the PL spectra in different solvents (**Figure S4**), showing clear broadening and red-shifted emission with the increasing solvent polarity.[37] PL emissions and the shift in different solvents both imply that **InCz23DMeTz** has the strongest ICT state and the lowest singlet energy.

Table 1. Thermal, photophysical, and energy levels of four compounds.

Compound.	T_d/T_g (°C) [a]	λ_{abs} (nm) [b]	λ_{em}/ FWHM (nm) [b]	HOMO/ LUMO [eV] [c]	HOMO/ LUMO [eV] [d]	Es/E_T [eV] [e]	ΔE_{ST} [eV] [f]	ΔE_{ST} [eV] [g]
InCz23FlTz	428/178	324, 364	432/57	-5.70/-2.85	-5.19/-1.93	2.94/2.75	0.19	0.252
InCz23DPhTz	463/-	308, 366	442/69	-5.51/-2.88	-5.21/-1.95	2.91/2.74	0.17	0.253
InCz23DMeTz	374/170	309, 362	456/79	-5.48/-2.90	-5.16/-1.96	2.87/2.72	0.15	0.232
InCz34DPhTz	436/181	315, 372	446/73	-5.47/-2.86	-5.12/-1.98	2.90/2.79	0.11	0.210

[a] T_d and T_g were obtained from TGA and DSC measurements; [b] in toluene solution; [c] energy levels from the redox potential in CV; [d] calculated from DFT; [e] S_1 energy estimated from the onset of the fluorescence spectra of 10% w/w compound in DPEPO at 300 K, and T_1 obtained from the onset of phosphorescence spectra of 10% w/w compound in DPEPO at 80 K; [f] Energy gap between S_1 and T_1; [g] Calculated S_1 and T_1 energy gaps by TDDFT.

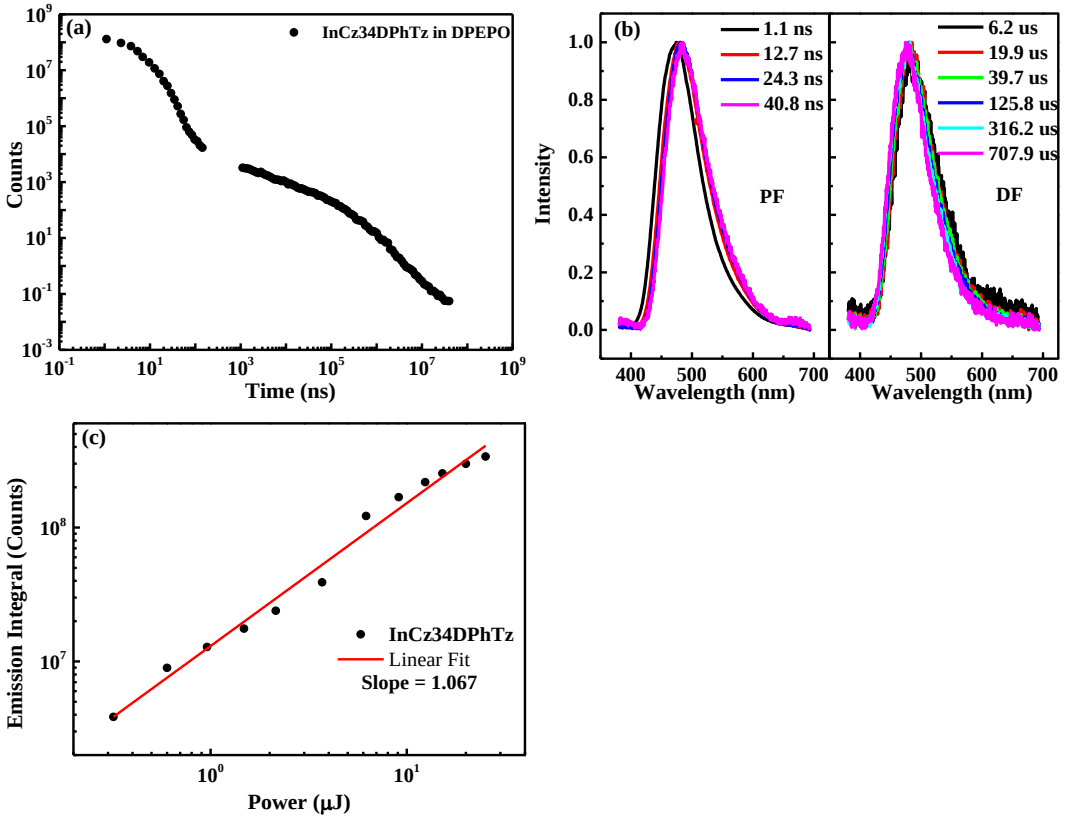

Figure 3. (a) Emission intensity against delay time measured at 300 K of 10% w/w **InCz34DPhTz** in DPEPO; (b) Normalized time resolved emission spectra, obtained in 10% w/w **InCz34DPhTz** in DPEPO film at 300 K; (c) DF linear dependence with excitation power of **InCz34DPhTz** doped in DPEPO.

The steady state emission spectra of degassed (prompt + delayed) emission, and aerated (prompt emission only), of the four compounds in zeonex matrix, are compared in **Figure S5**. Zeonex was used because it has a similar polarity to non-polar solvents such as methyl cyclohexane, whereas poly-(methyl methacrylate)

(PMMA) has a higher polarity.[38] As CT states would be stabilized in polar media, by using zeonex as host, there is no 'solvent' reorientation and the CT energy and the molecular structure of the guest are fixed.[39] In zeonex, therefore ^{1}CT of the emitters and the TADF properties can be studied without the influence of polarity. The largest contribution of delayed fluorescence is obtained in **InCz34DPhTz** (DF/PF=2.69). The other three compounds **InCz23FlTz** (DF/PF=0.22), **InCz23DPhTz** (DF/PF=0.29), and **InCz23DMeTz** (DF/PF=0.72), show relatively small DF contributions to the overall emission. However, the TADF contribution is clearly demonstrated in all compounds. The compounds substituted at 2, 3 positions show less TADF than the compound substituted at the 3, 4 position, which may be ascribed to the relatively larger ΔE_{ST} of 2, 3 substituted compounds.

As the excited-states of CT character are very sensitive to the host polarity, it is important that the photophysical properties of the blue emitters are characterized in the DPEPO (oxybis(2,1-phenylene))bis(diphenylphosphine oxide) host used in device fabrication. **Figure 3(a)** shows the time resolved emission decay curve of **InCz34DPhTz** in DPEPO at 300 K. Prompt fluorescence is observed at early times with a decay time constant of 3.3 ns, and delayed fluorescence decaying in the μs-ms range with a time constant of 70.3 μs. **Figure 3(b)**, shows the time dependent, normalized emission spectra in the PF and DF time range. In the PF region, the spectrum is red-shift due to the energy relaxation of ^{1}CT state. In contrast, the emission in the DF region shows a blue-shift with time. This probably occurs due to the presence of conformers with slightly different D-A torsional angles, which lead to the observation of different singlet-triplet gaps, and thus different RISC constants. The conformers with smaller $\Delta E_{ST,}$ probably those emitting in the red-region, which have the most relaxed conformation, suffer a more efficient RISC process and thus show faster DF decay than the bluer emitters, where the excited state is less relaxed, and RISC is slower. Over time the contribution of the emitters with bluer fluorescence starts to dominate and the spectrum shifts to shorter wavelengths. To sum up, the shifts in PF and DF part are both negligible, which demonstrates this little spectral

changes may just come from the torsional angle changes of the excited states instead the different conformations. The emission decays and time resolved spectra for the other three compounds are shown in SI (**Figure S6**). The PF lifetimes are in the range of 3.9-10.3 ns, and the DF lifetimes are between 77.0-97.9 μs. Furthermore, the intensity of the delayed fluorescence of **InCz34DPhTz** doped in DPEPO film, integrated from 1 μs to 7 ms, shows perfect linear relation with excitation power (gradient = 1 in log-log scale), clearly identifying the origin of the DF as a TADF process.[40-41] The phosphorescence spectra of all molecules in DPEPO films, recorded at 80 K are shown in **Figure S7**. All compounds show similar phosphorescence spectrum with a local triplet state character (^{3}LE) in DPEPO, however **InCz34DPhTz** shows a higher T_1 energy than the others due to the different conjugation degree. As for S_1, they were in the order of 2.94 eV (**InCz23FlTz**), 2.91 eV (**InCz23DPhTz**), 2.87 eV (**InCz23DMeTz**), 2.90 eV (**InCz34DPhTz**), which is in accordance with the strength of ICT states. Therefore, **InCz34DPhTz** maintains a higher T_1 and a relatively higher S_1 because of the comprehensive effect of steric influence and electron-donating abilities, and finally achieves the smallest energy gap between S_1 and T_1 among the four compounds (**Table1**). In addition, the other three compounds also exhibit linear DF dependence with excitation power (slopes are all near 1) as shown in **Figure S8**.

The fluorescence decays of the four compounds obtained in DPEPO films as a function of temperature are shown in **Figure 4**. Three emission regions are clearly identified in these decays. These are assigned to PF, DF and phosphorescence (Phos). All curves show a region of no emission after the decay of the prompt emission. This no emission window appears as a result of a slow RISC rate causing the emission to be too weak to be detected by the iCCD camera in our system. The emission decay is then followed by the DF emission regions all showing stronger intensity as temperature increases, thus demonstrating the TADF process. Finally, at later times, phosphorescence emission is also observed. As expected, phosphorescence shows stronger intensity at lower temperatures, in clear contrast with the DF.[40]

It is clearly that the contributions of TADF are small for all the four compounds, and **InCz34DPhTz** has a larger proportion of DF and a smaller non-emission interval than the other three compounds, which faster RISC process. From the PF and DF contributions in the decay curves, the DF quantum efficiencies (Φ_d) were estimated as 8.0-16.0%, and the PF quantum efficiencies (Φ_P) of all the four compounds are determined as 60.0-72.6%, owing to their larger radiative transition probability. The rate constants of PF (k_{PF}), DF (k_{TADF}), ISC (k_{ISC}) and RISC (k_{RISC}) are calculated at 300 K and summarized in **Table 2**.[42-43] As expected the k_{RISC} is relatively slow and ranges from 9.5~17.2×10^3 s^{-1}. Interestingly, the k_{PF} in **InCz34DPhTz** is almost 2.2×10^8 s^{-1}, which is consistent with the excellent EL performance of this compound. The faster PF lifetime is also important to reduce singlet singlet annihilation (SSA) processes.[44]

Table 2. photophysical constants.

compound	τ_p [a] (ns)	τ_d [a] (μs)	Φ_P [b] (%)	Φ_d [b] (%)	Φ_{PL} [c] (%)	k_{RISC} (10^4 s^{-1})	k_F (10^8 s^{-1})	λ_{PL} [d] (nm)	k_{TADF} (10^4 s^{-1})
InCz23FlTz	3.9	97.9	70.3	15.3	85.6	1.17	1.80	470	0.87
InCz23DPhTz	10.3	86.6	79.1	12.0	91.1	1.26	0.77	471	1.05
InCz23DMeTz	9.3	77.0	76.8	16.5	93.3	1.57	0.83	488	1.21
InCz34DPhTz	3.3	70.3	86.7	11.2	97.9	1.60	2.63	475	1.39

a) τ_P (the prompt lifetime) and τ_d (the delayed lifetime) were obtained from transient PL decay of doped films (10% in DPEPO host); b) Φ_P (the PF contribution to the overall emission) and Φ_d (the DF contribution to the overall emission) were estimated according to the prompt and delayed proportions in transient decay curves; c) Absolute PLQY of compounds doped in DPEPO films measured with integrating sphere under nitrogen atmosphere; d) the emission peaks of doped films.

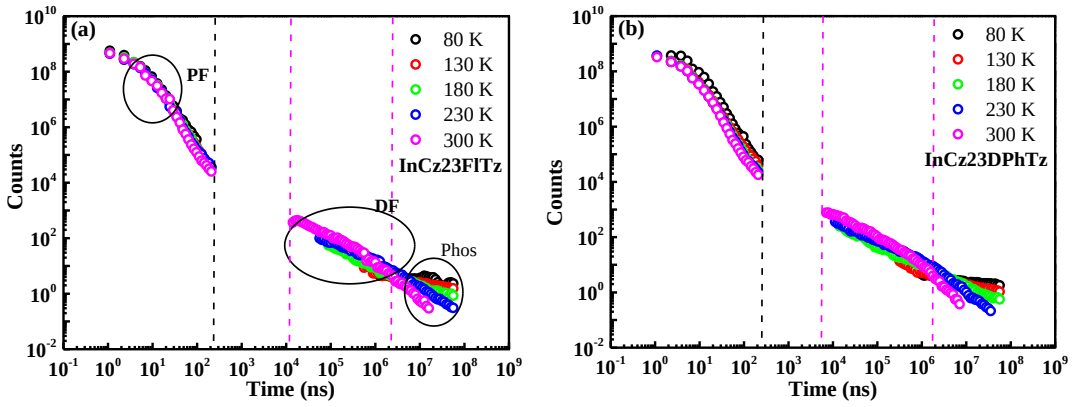

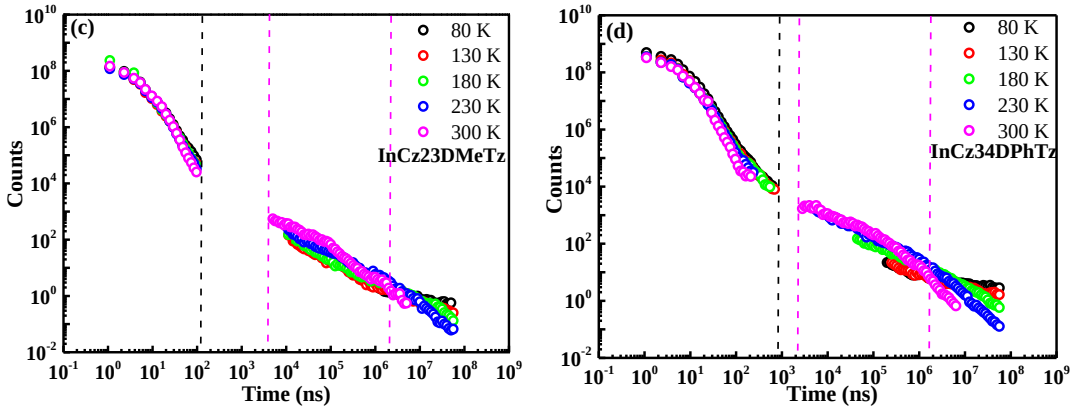

Figure 4. Temperature dependence of four compounds fluorescence decays.

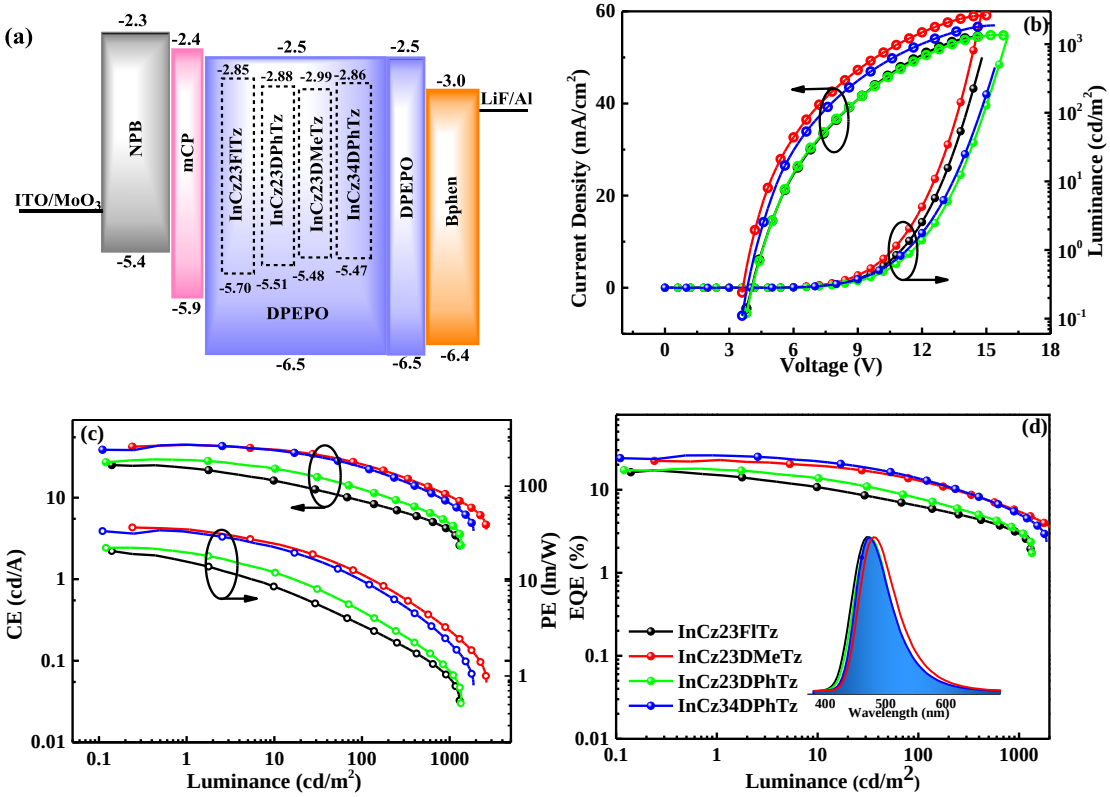

Figure 5. The EL performance of the four compounds.

compound	V_{on}[a] (V)	CE[b] (cd/A)	PE[b] (lm/W)	EQE[b] (%)	CIE[c]	EL[c] (nm)
InCz23FlTz	4.5	25.1/9.0/4.1	20.7/3.4/1.0	17.2/6.4/3.1	(0.15, 0.18)	468
InCz23DPhTz	4.5	29.4/12.4/4.8	22.5/4.6/1.1	17.9/8.1/3.2	(0.15, 0.22)	472
InCz23DMeTz	4.0	44.4/26.1/10.6	34.8/12.1/3.1	22.8/13.1/5.6	(0.16, 0.30)	480
InCz34DPhTz	4.3	44.6/24.5/8.9	34.3/10.7/2.4	25.9/14.2/5.3	(0.15, 0.24)	472

[a.] turn-on voltage (at a brightness of 1 cd m^{-2});[b.] the maximum CE (current efficiency), PE (power efficiency) and EQE (external quantum efficiency), and CE, PE, EQE at 100 cd $m^{-2}$and 1000 cd m^{-2}

[c.] CIE: Commission Internationale de l'Eclairage chromaticity coordinates at 100 cd m^{-2}.

Devices. In order to evaluate the potential of the four emitters in TADF OLEDs, prototype devices were made with the following structures: ITO/MoO_3 (10 nm)/NPB (70-80 nm)/mCP (15-20 nm)/DPEPO: 10% **InCz23FlTz/**or **InCz23DPhTz/**or **InCz23DMeTz/**or **InCz34DPhTz** (25 nm)/DPEPO (10-15 nm)/BPhen (30-40 nm)/LiF (1 nm)/Al; Each layer was optimized to get a better performance for each compounds and the structures of every functional material are presented in **Table S2**. MoO_3 and LiF worked as hole and electron-injecting layers, 4,4'-bis[*N*-(1-naphthyl)-*N*-phenylamino]-1,1'-biphenyl (NPB) and bathophenanthroline (BPhen) served as hole- and electron-transporting layers (HTL and ETL), and 1,3-bis(N-carbazolyl)benzene (*m*CP) was used as exciton-blocking layer and DPEPO was taken as the host material and exciton blocking layer, respectively (**Figure 5a**). The detailed structures of these devices and the used materials are listed in **Table S2**. As seen in **Figure 5b**, the turn-on voltage is about 4.0-4.5 V, which is consistent with other TADF emitters. Inspiringly, **InCz34DPhTz** realized a maximum EQE about 25.9 %, a maximum current efficiency (CE) of 44.6 cd/A and a maximum power efficiency (PE) of 34.3 lm/W, with CIE coordinates of (0.15, 0.24), confirming this to be a blue emitting device. Considering the optical properties discussed above, **InCz34DPhTz** has the most efficient triplet harvesting character compared to the other three,[45] and even the PLQY and RISC rate are weaker and slower for **InCz23FlTz**, **InCz23DPhTz** and **InCz23DMeTz**. Therefore, the best performance of **InCz34DPhTz** confirms the spectrosocopy data. However, the other compounds also realized devices with maximum EQE clearly above 10%, 17.2%, 17.9% and 22.8% respectively, and all with emission in the blue region,, with EL peaks at 468~ 480 nm as shown in **Figure 5d**. Unfortunately, the efficiencies decrease to 6.4%, 8.1%, 13.1%, 14.2% at 100 $cd.m^{-2}$ for **InCz23FlTz**, **InCz23DPhTz**, **InCz23DMeTz** and **InCz34DPhTz** respectively, and drop further to 3.1%, 3.2%, 5.6% and 5.3% at 1000cdm^{-2}. The efficiency roll-off is thus not negligible. We assign this drop-off in efficiency to TTA (triplet–triplet annihilation), however TPA (triplet-polaron annihilation) and STA (singlet-triplet annihilation) may also

contribute. These effects are promoted by the long lifetime of the triplet state as a result of the slow RISC rate. Fittings of the current intensity and EQE curves with TTA model (as shown in **Figure S9**),[46-48] show that in devices B and D TTA is the dominant process leading to the efficiency roll-off in **InCz23DMeTz** and **InCz34DPhTz** devices. On the other hand, devices A and C showing lower EQE at about 17% have much derivation for TTA mode, which may attribute to the lower triplet exciton density in the emitting layer.[49] Besides, DPEPO might also cause imbalanced charge transfer, which would aggravate the efficiency roll-off. As seen in Figure S10, the ^{1}LE is estimated by the emission in n-hexane, and the ^{1}CT and ^{3}LE are obtained from the emission of doped films in DPEPO host, which is in accordance with the emission layer of devices. It was found that all the compounds show mixed triplet state of ^{3}LE and ^{3}CT from the theoretical calculations, and the hyperfine coupling between ^{1}CT and ^{3}CT states would not occur unless the energy difference is smaller than 20 μeV.[50] Here, maybe ^{3}CT can reserve the triplet energy, and the main mechanism of triplet to singlet is the SOC of ^{3}LE to ^{1}CT. Despite the efficiency roll-off, our results confirm that devices of good performance can be obtained even with materials that show slow RISC rate, if triplet harvesting is counterbalanced by a strong radiative process, as it is observed in the materials studied here.

■ Conclusion

In summary, a series of blue emitters were designed and synthesized based on indenocarbazole-derived compounds. A systematic study of the effect of different substituents and substitution positions of the donors on their photophysical behavior and electroluminescence performances were carry out. The four studied compounds, **InCz23FlTz, InCz23DPhTz, InCz23DMeTz** and **InCz34DPhTz**, show strong PLQY in doped DPEPO films that range from 85.6-97.9 % due to the rigid structures. They also show relatively small TADF contribution under optical excitation, due to the relatively large gap between singlet and triplet (~0.2 eV) and slow reverse intersystem crossing rate (~10^{4} s^{-1}). In spite of this, the compounds performed very well in electroluminescence devices. Especially, **InCz34DPhTz** with the shortest

delayed lifetime and the highest PLQY among the four compounds, showing a maximum EQE around 26%, with no enhancement of light outcoupling. It is thus concluded that the modification on the substituted position of carbazole and substituents can adjust the color purity and TADF properties to obtain good EL performance finally.

AUTHOR INFORMATION

Corresponding Author

*E-mail: wanglei@mail.hust.edu.cn

*E-mail: f.m.b.dias@durham.ac.uk

Notes

The authors declare no competing financial interest.

ACKNOWLEDGMENT

This research work was supported by the NSFC/China (51573065, 51727809), China Postdoctoral Science Foundation (2017M620321), the science and technology support program of Hubei Province (2015BAA075). Thanks to SCTS/CGCL HPCC of HUST for providing computing resources and technical support. The Analytical and Testing Center at Huazhong University of Science and Technology is acknowledged for characterization of new compounds. FMBD thanks The Royal Society, UK for the funding, IEC\NSFC\170130 - International Exchanges 2017 Cost Share (China).

REFRENCES

(1) Yang, Z.; Mao, Z.; Xie, Z.; Zhang, Y.; Liu, S.; Zhao, J.; Xu, J.; Chi, Z.; Aldred, M. P. Recent advances in organic thermally activated delayed fluorescence materials. *Chem. Soc. Rev.* **2017,** *46* (3), 915-1016, DOI: 10.1039/c6cs00368k.

(2) Wong, M. Y.; Zysman-Colman, E. Purely Organic Thermally Activated Delayed Fluorescence Materials for Organic Light-Emitting Diodes. *Adv. Mater.* **2017,**

1605444, DOI: 10.1002/adma.201605444.

(3) Im, Y.; Byun, S. Y.; Kim, J. H.; Lee, D. R.; Oh, C. S.; Yook, K. S.; Lee, J. Y. Recent Progress in High-Efficiency Blue-Light-Emitting Materials for Organic Light-Emitting Diodes. *Adv. Funct. Mater.* **2017,** *1603007*, DOI: 10.1002/adfm.201603007.

(4) Song, W.; Lee, J. Y. Degradation Mechanism and Lifetime Improvement Strategy for Blue Phosphorescent Organic Light-Emitting Diodes. *Adv. Optical Mater.* **2017,** *5* (9), 1600901, DOI: 10.1002/adom.201600901.

(5) Cui, L. S.; Deng, Y. L.; Tsang, D. P.; Jiang, Z. Q.; Zhang, Q.; Liao, L. S.; Adachi, C. Controlling Synergistic Oxidation Processes for Efficient and Stable Blue Thermally Activated Delayed Fluorescence Devices. *Adv. Mater.* **2016,** *28* (35), 7620-5, DOI: 10.1002/adma.201602127.

(6) Li, Y.; Liang, J.-J.; Li, H.-C.; Cui, L.-S.; Fung, M.-K.; Barlow, S.; Marder, S. R.; Adachi, C.; Jiang, Z.-Q.; Liao, L.-S. The role of fluorine-substitution on the π-bridge in constructing effective thermally activated delayed fluorescence molecules. *J. Mater. Chem. C* **2018,** *6* (20), 5536-5541, DOI: 10.1039/c8tc01158c.

(7) Ahn, D. H.; Jeong, J. H.; Song, J.; Lee, J. Y.; Kwon, J. H. Highly Efficient Deep Blue Fluorescent Organic Light-Emitting Diodes Boosted by Thermally Activated Delayed Fluorescence Sensitization. *ACS Appl. Mater. Interfaces* **2018,** *10* (12), 10246-10253, DOI: 10.1021/acsami.7b19030.

(8) Sarma, M.; Wong, K. T. Exciplex: An Intermolecular Charge-Transfer Approach for TADF. *ACS Appl. Mater. Interfaces* **2018**, DOI: 10.1021/acsami.7b18318.

(9) Dias, F. B.; Penfold, T. J.; Monkman, A. P. Photophysics of thermally activated delayed fluorescence molecules. *Methods Appl Fluoresc* **2017,** *5* (1), 012001, DOI: 10.1088/2050-6120/aa537e.

(10) Park, I. S.; Matsuo, K.; Aizawa, N.; Yasuda, T. High-Performance Dibenzoheteraborin-Based Thermally Activated Delayed Fluorescence Emitters: Molecular Architectonics for Concurrently Achieving Narrowband Emission and Efficient Triplet-Singlet Spin Conversion. *Adv. Funct. Mater.* **2018**, 1802031, DOI:

10.1002/adfm.201802031.

(11) Huang, W.; Einzinger, M.; Zhu, T.; Chae, H. S.; Jeon, S.; Ihn, S.-G.; Sim, M.; Kim, S.; Su, M.; Teverovskiy, G.; Wu, T.; Van Voorhis, T.; Swager, T. M.; Baldo, M. A.; Buchwald, S. L. Molecular Design of Deep Blue Thermally Activated Delayed Fluorescence Materials Employing a Homoconjugative Triptycene Scaffold and Dihedral Angle Tuning. *Chem. Mater.* **2018,** *30* (5), 1462-1466, DOI: 10.1021/acs.chemmater.7b03490.

(12) Im, Y.; Kim, M.; Cho, Y. J.; Seo, J.-A.; Yook, K. S.; Lee, J. Y. Molecular Design Strategy of Organic Thermally Activated Delayed Fluorescence Emitters. *Chem. Mater.* **2017,** *29* (5), 1946-1963, DOI: 10.1021/acs.chemmater.6b05324.

(13) Kim, J. H.; Yun, J. H.; Lee, J. Y. Recent Progress of Highly Efficient Red and Near-Infrared Thermally Activated Delayed Fluorescent Emitters. *Adv. Optical Mater.* **2018**, 1800255, DOI: 10.1002/adom.201800255.

(14) Wex, B.; Kaafarani, B. R. Perspective on carbazole-based organic compounds as emitters and hosts in TADF applications. *J. Mater. Chem. C* **2017,** *5* (34), 8622-8653, DOI: 10.1039/c7tc02156a.

(15) Rajamalli, P.; Senthilkumar, N.; Gandeepan, P.; Ren-Wu, C. C.; Lin, H. W.; Cheng, C. H. A Method for Reducing the Singlet-Triplet Energy Gaps of TADF Materials for Improving the Blue OLED Efficiency. *ACS Appl. Mater. Interfaces* **2016,** *8* (40), 27026-27034, DOI: 10.1021/acsami.6b10678.

(16) Guo, K. P.; Wang, H. D.; Wang, Z. X.; Si, C. F.; Peng, C. Y.; Chen, G.; Zhang, J. H.; Wang, G. F.; Wei, B. Stable green phosphorescence organic light-emitting diodes with low efficiency roll-off using a novel bipolar thermally activated delayed fluorescence material as host. *Chem. Sci.* **2017,** *8* (2), 1259-1268, DOI: 10.1039/c6sc03008d.

(17) Ryoo, C. H.; Cho, I.; Han, J.; Yang, J. H.; Kwon, J. E.; Kim, S.; Jeong, H.; Lee, C.; Park, S. Y. Structure-Property Correlation in Luminescent Indolo[3,2-b]indole (IDID) Derivatives: Unraveling the Mechanism of High Efficiency Thermally Activated Delayed Fluorescence (TADF). *ACS Appl. Mater. Interfaces* **2017**, DOI:

10.1021/acsami.7b13158.

(18) Zhang, D.; Zhao, C.; Zhang, Y.; Song, X.; Wei, P.; Cai, M.; Duan, L. Highly Efficient Full-Color Thermally Activated Delayed Fluorescent Organic Light-Emitting Diodes: Extremely Low Efficiency Roll-Off Utilizing a Host with Small Singlet-Triplet Splitting. *ACS Appl. Mater. Interfaces* **2017,** *9* (5), 4769-4777, DOI: 10.1021/acsami.6b15272.

(19) Dongdong Zhang, X. S., Minghan Cai, Hironori Kaji, and Lian Duan*. Versatile Indolocarbazole-Isomer Derivatives as Highly Emissive Emitters and Ideal Hosts for Thermally Activated Delayed Fluorescent OLEDs with Alleviated Efficiency Roll-Off. *Adv. Mater.* **2018**, DOI: 10.1002/adma.201705406.

(20) Kim, K. J.; Kim, G. H.; Lampande, R.; Ahn, D. H.; Im, J. B.; Moon, J. S.; Lee, J. K.; Lee, J. Y.; Lee, J. Y.; Kwon, J. H. A new rigid diindenocarbazole donor moiety for high quantum efficiency thermally activated delayed fluorescence emitter. *J. Mater. Chem. C* **2018**, DOI: 10.1039/c7tc04852a.

(21) Zhu, X.-D.; Tian, Q.-S.; Zheng, Q.; Wang, Y.-K.; Yuan, Y.; Li, Y.; Jiang, Z.-Q.; Liao, L.-S. Deep-blue thermally activated delayed fluorescence materials with high glass transition temperature. *J. Lumin.* **2019,** *206*, 146-153, DOI: 10.1016/j.jlumin.2018.10.017.

(22) Lv, X. Z., W.; Ding, D.; Han, C.; Huang, Z.; Xiang, S.; Zhang, Q.; Xu, H.; Wang, L. Integrating the Emitter and Host Characteristics of Donor–Acceptor Systems through Edge-Spiro Effect Toward 100%Exciton Harvesting in Blue and White Fluorescence Diodes. *Adv. Optical Mater.* **2018,** *6* (12), 1800165, DOI: 10.1002/adom.201800165.

(23) Wang, K.; Zheng, C. J.; Liu, W.; Liang, K.; Shi, Y. Z.; Tao, S. L.; Lee, C. S.; Ou, X. M.; Zhang, X. H. Avoiding Energy Loss on TADF Emitters: Controlling the Dual Conformations of D-A Structure Molecules Based on the Pseudoplanar Segments. *Adv. Mater.* **2017**, DOI: 10.1002/adma.201701476.

(24) Chen, D. G.; Lin, T. C.; Chen, C. L.; Chen, Y. T.; Chen, Y. A.; Lee, G. H.; Chou, P. T.; Liao, C. W.; Chiu, P. C.; Chang, C. H.; Lien, Y. J.; Chi, Y. Optically Triggered

Planarization of Boryl-Substituted Phenoxazine: Another Horizon of TADF Molecules and High-Performance OLEDs. *ACS Appl. Mater. Interfaces* **2018,** *10* (15), 12886-12896, DOI: 10.1021/acsami.8b00053.

(25) dos Santos, P. L.; Ward, J. S.; Batsanov, A. S.; Bryce, M. R.; Monkman, A. P. Optical and Polarity Control of Donor–Acceptor Conformation and Their Charge-Transfer States in Thermally Activated Delayed-Fluorescence Molecules. *J. Phys. Chem. C* **2017,** *121* (30), 16462-16469, DOI: 10.1021/acs.jpcc.7b03672.

(26) Kim, M.; Jeon, S. K.; Hwang, S. H.; Lee, J. Y. Stable blue thermally activated delayed fluorescent organic light-emitting diodes with three times longer lifetime than phosphorescent organic light-emitting diodes. *Adv. Mater.* **2015,** *27* (15), 2515-20, DOI: 10.1002/adma.201500267.

(27) Lv, X.; Zhang, W.; Ding, D.; Han, C.; Huang, Z.; Xiang, S.; Zhang, Q.; Xu, H.; Wang, L. Integrating the Emitter and Host Characteristics of Donor-Acceptor Systems through Edge-Spiro Effect Toward 100% Exciton Harvesting in Blue and White Fluorescence Diodes. *Adv. Optical Mater.* **2018**, 1800165, DOI: 10.1002/adom.201800165.

(28) Shizu, K.; Noda, H.; Tanaka, H.; Taneda, M.; Uejima, M.; Sato, T.; Tanaka, K.; Kaji, H.; Adachi, C. Highly Efficient Blue Electroluminescence Using Delayed-Fluorescence Emitters with Large Overlap Density between Luminescent and Ground States. *J. Phys. Chem. C* **2015,** *119* (47), 26283-26289, DOI: 10.1021/acs.jpcc.5b07798.

(29) Cai, X.; Su, S.-J. Marching Toward Highly Efficient, Pure-Blue, and Stable Thermally Activated Delayed Fluorescent Organic Light-Emitting Diodes. *Adv. Funct. Mater.* **2018**, 1802558, DOI: 10.1002/adfm.201802558.

(30) Wang, S.; Cheng, Z.; Song, X.; Yan, X.; Ye, K.; Liu, Y.; Yang, G.; Wang, Y. Highly Efficient Long-Wavelength Thermally Activated Delayed Fluorescence OLEDs Based on Dicyanopyrazino Phenanthrene Derivatives. *ACS Appl. Mater. Interfaces* **2017**, DOI: 10.1021/acsami.6b14796.

(31) Dos Santos, P. L.; Ward, J. S.; Congrave, D. G.; Batsanov, A. S.; Eng, J.; Stacey,

J. E.; Penfold, T. J.; Monkman, A. P.; Bryce, M. R. Triazatruxene: A Rigid Central Donor Unit for a D-A3 Thermally Activated Delayed Fluorescence Material Exhibiting Sub-Microsecond Reverse Intersystem Crossing and Unity Quantum Yield via Multiple Singlet-Triplet State Pairs. *Adv Sci* **2018,** *5* (6), 1700989, DOI: 10.1002/advs.201700989.

(32) Dias, F. B.; Santos, J.; Graves, D. R.; Data, P.; Nobuyasu, R. S.; Fox, M. A.; Batsanov, A. S.; Palmeira, T.; Berberan-Santos, M. N.; Bryce, M. R.; Monkman, A. P. The Role of Local Triplet Excited States and D-A Relative Orientation in Thermally Activated Delayed Fluorescence: Photophysics and Devices. *Advanced Science* **2016**, 1600080, DOI: 10.1002/advs.201600080.

(33) Dias, F. B.; Bourdakos, K. N.; Jankus, V.; Moss, K. C.; Kamtekar, K. T.; Bhalla, V.; Santos, J.; Bryce, M. R.; Monkman, A. P. Triplet harvesting with 100% efficiency by way of thermally activated delayed fluorescence in charge transfer OLED emitters. *Adv. Mater.* **2013,** *25* (27), 3707-14, DOI: 10.1002/adma.201300753.

(34) Takuya Hosokai, 2* Hiroyuki Matsuzaki,1,2 Hajime Nakanotani,3,4* Katsumi Tokumaru,2 Tetsuo Tsutsui,2 Akihiro Furube,1,2† Keirou Nasu,5 Hiroko Nomura,5 Masayuki Yahiro,6 Chihaya Adachi. Evidence and mechanism of efficient thermally activated delayed fluorescence promoted by delocalized excited states. *Science Advances* **2017,** *3*, 1603282, DOI: 10.1126/sciadv.1603282.

(35) Wada, Y.; Kubo, S.; Kaji, H. Adamantyl Substitution Strategy for Realizing Solution-Processable Thermally Stable Deep-Blue Thermally Activated Delayed Fluorescence Materials. *Adv. Mater.* **2018**, DOI: 10.1002/adma.201705641.

(36) Lien, Y. J.; Lin, T. C.; Yang, C. C.; Chiang, Y. C.; Chang, C. H.; Liu, S. H.; Chen, Y. T.; Lee, G. H.; Chou, P. T.; Lu, C. W.; Chi, Y. First N-Borylated Emitters Displaying Highly Efficient Thermally Activated Delayed Fluorescence and High-Performance OLEDs. *ACS Appl. Mater. Interfaces* **2017,** *9* (32), 27090-27101, DOI: 10.1021/acsami.7b08258.

(37) Legaspi, C. M.; Stubbs, R. E.; Wahadoszaman, M.; Yaron, D. J.; Peteanu, L. A.; Kemboi, A.; Fossum, E.; Lu, Y.; Zheng, Q.; Rothberg, L. J. Rigidity and Polarity

Effects on the Electronic Properties of Two Deep Blue Delayed Fluorescence Emitters. *J. Phys. Chem. C* **2018,** *122* (22), 11961-11972, DOI: 10.1021/acs.jpcc.7b12025.

(38) Matulaitis, T.; Imbrasas, P.; Kukhta, N. A.; Baronas, P.; Bučiūnas, T.; Banevičius, D.; Kazlauskas, K.; Gražulevičius, J. V.; Juršėnas, S. Impact of Donor Substitution Pattern on the TADF Properties in the Carbazolyl-Substituted Triazine Derivatives. *J. Phys. Chem. C* **2017,** *121* (42), 23618-23625, DOI: 10.1021/acs.jpcc.7b08034.

(39) Etherington, M. K.; Gibson, J.; Higginbotham, H. F.; Penfold, T. J.; Monkman, A. P. Revealing the spin-vibronic coupling mechanism of thermally activated delayed fluorescence. *Nat. Commun.* **2016,** *7*, 13680, DOI: 10.1038/ncomms13680.

(40) Dos Santos, P. L.; Ward, J. S.; Bryce, M. R.; Monkman, A. P. Using Guest-Host Interactions To Optimize the Efficiency of TADF OLEDs. *J Phys Chem Lett* **2016,** *7* (17), 3341-6, DOI: 10.1021/acs.jpclett.6b01542.

(41) Dias, F. B. Kinetics of thermal-assisted delayed fluorescence in blue organic emitters with large singlet-triplet energy gap. *Philosophical transactions. Series A, Mathematical, physical, and engineering sciences* **2015,** *373* (2044), DOI: 10.1098/rsta.2014.0447.

(42) Shizu, K.; Tanaka, H.; Uejima, M.; Sato, T.; Tanaka, K.; Kaji, H.; Adachi, C. Strategy for Designing Electron Donors for Thermally Activated Delayed Fluorescence Emitters. *J. Phys. Chem. C* **2015,** *119* (3), 1291-1297, DOI: 10.1021/jp511061t.

(43) Hatakeyama, T.; Shiren, K.; Nakajima, K.; Nomura, S.; Nakatsuka, S.; Kinoshita, K.; Ni, J.; Ono, Y.; Ikuta, T. Ultrapure Blue Thermally Activated Delayed Fluorescence Molecules: Efficient HOMO-LUMO Separation by the Multiple Resonance Effect. *Adv. Mater.* **2016,** *28* (14), 2777-81, DOI: 10.1002/adma.201505491.

(44) Liu, Z.; Cao, F.; Tsuboi, T.; Yue, Y.; Deng, C.; Ni, X.; Sun, W.; Zhang, Q. High Fluorescence Rate as a Key for Stable Blue Organic Light-Emitting Diodes. *J. Mater. Chem. C* **2018**, DOI: 10.1039/c8tc01471j.

(45) Nakanotani, H.; Higuchi, T.; Furukawa, T.; Masui, K.; Morimoto, K.; Numata,

M.; Tanaka, H.; Sagara, Y.; Yasuda, T.; Adachi, C. High-efficiency organic light-emitting diodes with fluorescent emitters. *Nat. Commun.* **2014,** *5*, 4016, DOI: 10.1038/ncomms5016.

(46) Masui, K.; Nakanotani, H.; Adachi, C. Analysis of exciton annihilation in high-efficiency sky-blue organic light-emitting diodes with thermally activated delayed fluorescence. *Org. Electron.* **2013,** *14* (11), 2721-2726, DOI: 10.1016/j.orgel.2013.07.010.

(47) Cai, X.; Gao, B.; Li, X.-L.; Cao, Y.; Su, S.-J. Singlet-Triplet Splitting Energy Management via Acceptor Substitution: Complanation Molecular Design for Deep-Blue Thermally Activated Delayed Fluorescence Emitters and Organic Light-Emitting Diodes Application. *Adv. Funct. Mater.* **2016,** *26* (44), 8042-8052, DOI: 10.1002/adfm.201603520.

(48) Wang, Y.-K.; Li, S.-H.; Wu, S.-F.; Huang, C.-C.; Kumar, S.; Jiang, Z.-Q.; Fung, M.-K.; Liao, L.-S. Tilted Spiro-Type Thermally Activated Delayed Fluorescence Host for ≈100% Exciton Harvesting in Red Phosphorescent Electronics with Ultralow Doping Ratio. *Adv. Funct. Mater.* **2018,** *28* (13), 1706228, DOI: 10.1002/adfm.201706228.

(49) Zhang, Q.; Wang, B.; Tan, J.; Mu, G.; Yi, W.; Lv, X.; Zhuang, S.; liu, w.; Wang, L. Optimized electron-transport material basing on m-terphenyl-diphenylphosphine oxide with harmonious compatibility of high ET and electron mobility for highly efficient OLEDs. *J. Mater. Chem. C* **2017**, DOI: 10.1039/c7tc02459b.

(50) Nobuyasu, R. S.; Ren, Z.; Griffiths, G. C.; Batsanov, A. S.; Data, P.; Yan, S.; Monkman, A. P.; Bryce, M. R.; Dias, F. B. Rational Design of TADF Polymers Using a Donor-Acceptor Monomer with Enhanced TADF Efficiency Induced by the Energy Alignment of Charge Transfer and Local Triplet Excited States. *Adv. Optical Mater.* **2016,** *4* (4), 597-607, DOI: 10.1002/adom.201500689.

Table of Contents